Journal of Power Sources, 40 (1992) 149–156

Scanning tunneling microscopy of lead dioxide

R. S. Robinson
Bell Communications Research, 331 Newman Springs Road, 3Z-275, Red Bank, NJ 07701 (USA)

Abstract

Scanning tunneling microscopy (STM) has become a superb tool for *in situ* electrochemical studies, because it provides extremely high resolution, real-space images of surface structure. We are using STM to study the growth morphology of lead dioxide, and to develop methods for determining the internal microstructure of the material. We have found that lead dioxide has a self-similar (fractal) grain structure from the nanometer to the micrometer scale. Knowledge of the effects of chemical environment and electrochemical deposition conditions on this morphology will lead to better understanding of the properties of lead dioxide as battery electrode material. To determine internal microstucture, STM is used to record structural features which emerge during chemical or electrochemical etching of a thick (hundreds of monolayers) deposit. These features represent internal layers which are successively 'peeled' back by the etching process. The images can be combined to form a three-dimensional tomographic volume from which two-dimensional slices can be taken in any orientation. This gives spatial information with subnanometer resolution about the number density and connectivity of structural voids, which affect electrolyte diffusion and electrode strength. Our STM instrument has been optimized regarding image acquisition rate. This minimizes the effects of microscope drift and facilitates observing time-dependent surface phenomena. Fast image acquisition rates are important for depth profiling, because a large number of depth 'slices' are required, with low distortion from microscope drift; otherwise, it would be impossible to obtain the image registration needed for constructing tomographic etching profiles.

Introduction

In scanning tunneling microscopy (STM) [1, 2] an electrically-biased, conductive tip is used to provide extremely high-resolution, real-space images of surface structure. The microscope relies on electronic tunneling between two conductors separated by an insulating material. One conductor is fashioned in the shape of a sharp tip; an atomic-size protrusion on the tip provides a tunneling path between the conductors (Fig. 1). The magnitude of the tunneling current i is an exponential function of product of the tip-surface separation s and electron work function ψ. Small changes in s result in large changes in i, so only the atoms on the end of the probe, closest to the surface, are 'seen' by the tunneling electrons. Thus, the 'microtip' closest to the surface is automatically selected for tunneling, effectively reducing the electronic size of the probe to the size of a single atom. The typical values of s are 2 to 10 Å, i 100 pA to 4 nA. Negative feedback is used to position the probe in the direction normal to the surface, maintaining a constant tunneling current, while the tip is raster scanned laterally. The tip motion is controlled with piezoelectric transducers [1–3]. A record of the tip motion in three dimensions provides images of surface structure with angstrom lateral and picometer vertical resolution. Because of its high-resolution capability, and

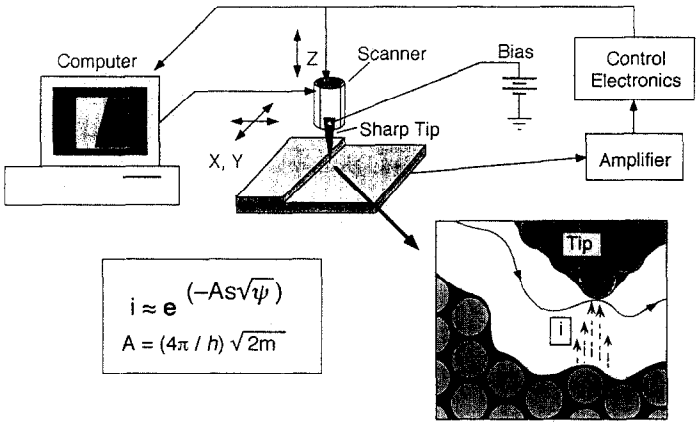

Fig. 1. Schematic diagram of a scanning tunneling microscope (STM). The tunneling current i is a logarithmic function of the electron work function ψ and tip-surface separation s (Å), h, Planck constant, m, electron mass.

the ability to examine surfaces immersed in many different environments, including electrolytes, STM has taken its place as a superb tool for surface electrochemical studies [4, 5]. Early reports also noted the promise of STM for investigations of surface electronic properties [2]. A number of such studies, conducted in vacuum or air [6], and recently in electrolyte [7], have since been published.

Because of the importance of lead dioxide as the major active component of the positive electrode in lead/acid batteries, we have made some preliminary measurements on electrodeposited PbO_2 films with STM. This material has been studied previously with STM [8]; however, our goal was the examination of PbO_2 *in situ*, in contact with electrolyte. Background current resulting from electrochemical processes between the tip and sample make *in situ* STM more difficult than STM in a nonelectrochemical environment; this is minimized by coating the tip with an insulating material. With proper coating, background currents can be reduced to less than 40 pA.

A primary failure mode of the positive electrode in a lead/acid battery is the oxidation and corrosion of the lead grid. This process is accelerated under conditions of electrode overcharge, when oxygen is evolved by electrolysis of water in the electrolyte. The grid corrosion rate may be influenced by the diffusion of O_2 to the grid surface. The diffusion rate is influenced by the internal microstructure of the electrode, ultimately controlled by the oxide layer near the grid surface, and the structure of this oxide likely evolves over the life of the battery.

Surface structural probes and transmission electron microscopy (TEM) give limited information about the microstructure inside the sample. However, we are developing a depth-profiling method for determining the internal structure of the deposit, based on *in situ* STM. The goal is a general method to examine the internal structure of electrochemically interesting materials, and a better understanding of the properties of PbO_2. If the surface of the material is monitored during dissolution in a mildly corrosive electrolyte, a series of images is obtained that represent cross sections taken through the sample, as the layers are 'peeled' back by the etching process. Quantitative dimensions in x, y, and z are provided by the STM. These cross sections can then be assembled into a three-dimensional tomographic volume. We envision using appropriate computer software to take two-dimensional slices in any orientation, giving an indication

about the number density and connectivity of structural voids, which affect electrolyte or gas diffusion and electrode strength. The density of voids can be estimated with TEM, but the connectivity of the voids, important to diffusion, cannot be determined with this technique. Since the major structural features of the oxide which can be monitored with the STM approach atomic dimensions, much of the structure of the deposit is preserved during the etching process, on the time scale of STM imaging.

Experimental

The substrates used for STM and electrochemistry were evaporated platinum on glass microscope slides, or 2 mm diameter platinum wire. The wire substrates were mechanically polished to a mirror finish (as inspected optically at magnification = 1000 with a metallurgical microscope) with 0.05 μm alumina, washed, then cycled 3 times between the platinum oxidation region and hydrogen evolution region in 1 M $HClO_4$ at 400 μA cm^2. To help exclude contaminants and maintain a reproducible sample environment, a stream of argon gas was passed through activated carbon and 200 nm membrane filters and directed through the STM scanner tube onto the sample. Lead dioxide was electrochemically deposited from 1.0 M $HClO_4$/0.8 M CH_3COOH/0.8 M $(CH_3COO)_2Pb$; this electrolyte was chosen because it allows preferential deposition of β-PbO_2 [8]. For the images of PbO_2 surfaces, the electrolyte was removed and the sample rinsed with distilled water and imaged while moistened with water, because electrodeposited PbO_2 dissolves in this electrolyte; we anticipate trying other electrolytes in the future. Dissolution experiments were performed with the sample at open circuit in the electrolyte.

The STM differs substantially from commercial instruments; details of its design are given elsewhere [5, 7, 9, 10]. The microscope tips were etched from 0.25 mm diameter iridium wire, and coated with Apiezon 'W' wax [7], or made from varnish-coated platinum–iridium obtained commercially (Longreach Scientific, Orr's Island, ME, USA). The free end of the STM tip must be short, a few mm, to keep the tip assembly rigid for good images. This constrains electrochemical experiments with flat substrates, because a thin layer of solution must be used, giving a small solution volume. However, with wire electrodes, the cell design shown in Fig. 2 permits a larger solution volume, reducing the possibility of solution contamination and changes in electrolyte concentration due to electrolysis or evaporation. To help identify possible artifacts, the images were recorded in both directions of tip motion in x (the fast scan direction) and y; the images shown here are bidirectionally (in x) scanned images, after correcting for piezoelectric distortions [10]. All images are shown displayed in a real-space, three-dimensional perspective.

Results and discussion

STM images of polished platinum electrodes at successively higher resolutions are shown in Figs. 3 to 6. The images demonstrate that even carefully-polished electrodes, which appear optically smooth, are quite rough on the STM measurement scale. This type of electrode is commonly used for electrochemical experiments, and the roughness on this distance scale could have important implications for ultrahigh-speed electrochemistry [11]. The trench-like feature in Fig. 5 has a width corresponding to the size of the finest polishing abrasive used, 50 nm. The portion of Fig. 5 indicated

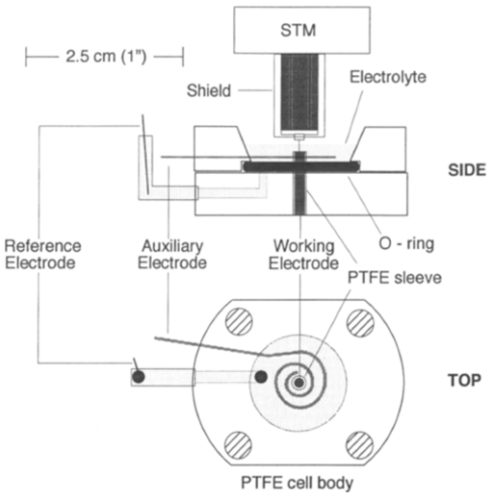

Fig. 2. Diagram of cell used for electrochemical STM experiments.

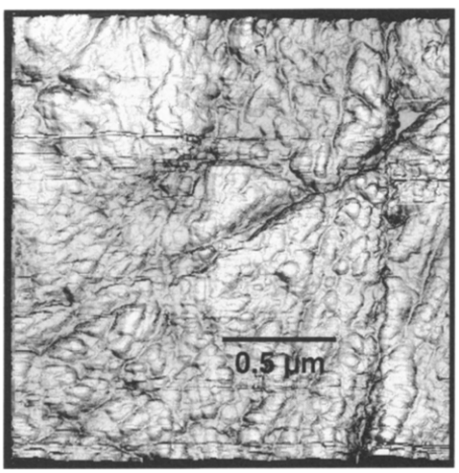

Fig. 3. Low-resolution STM image of polished platinum wire electrode.

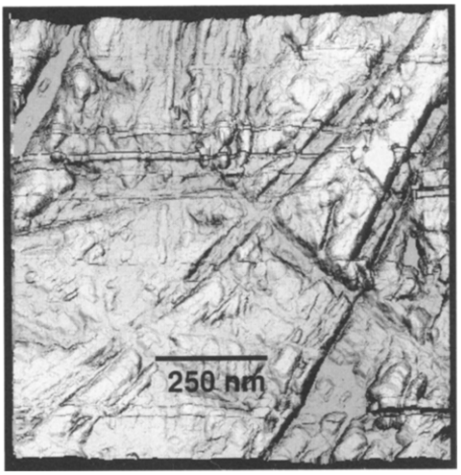

Fig. 4. STM image of polished platinum wire electrode.

by the dotted box was scanned at higher resolution and is displayed in Fig. 6. Here, individual atomic steps of platinum are resolved. To the author's knowledge, these are the first such images of polished samples in which atomic features are resolved. Images of a thick (400 monolayer) PbO_2 layer, deposited on the substrate, are shown in Fig. 7. The images in Figs. 7(a, b) were scanned at a tip bias of -1160 mV and 415 pA, while the remaining images of the same sample were scanned at slightly lower probe resolution (70 pA, tip further from surface) and -500 mV. These bias voltages gave the most stable tunneling, for the currents used. The fine, particulate-appearing features at the grain edges in Fig. 7(c) are possibly imaging artifacts, due to probe electronic effects [12]. The grain structure visible in Fig. 7(a) is faintly discernible in the lower right portion of Fig. 7(c). At lower resolution (Figs. 7(e, f), larger grains

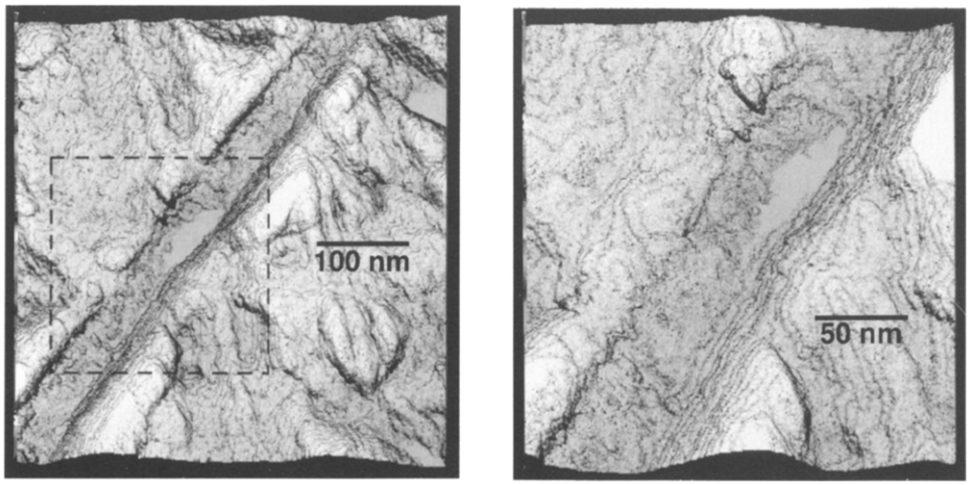

Fig. 5. STM image of polished platinum wire electrode; the box enclosed by the dotted line is shown at higher resolution in Fig. 6.

Fig. 6. High-resolution STM image of polished platinum wire electrode; terraces of platinum atoms are resolved.

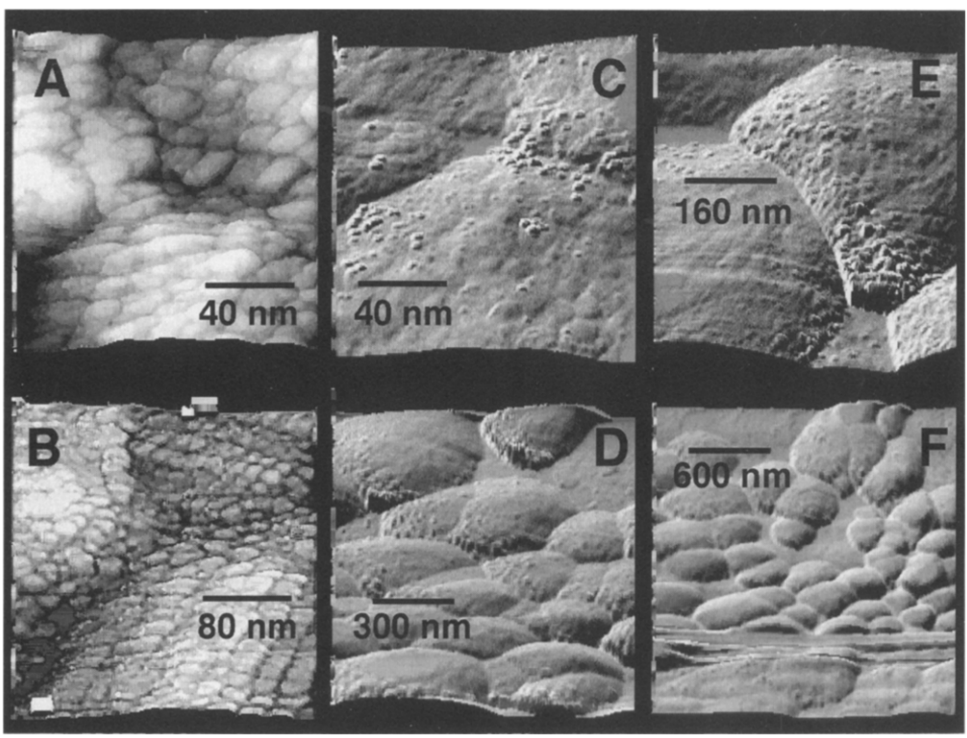

Fig. 7. STM image, obtained in air, of freshly-deposited, moist PbO_2 film.

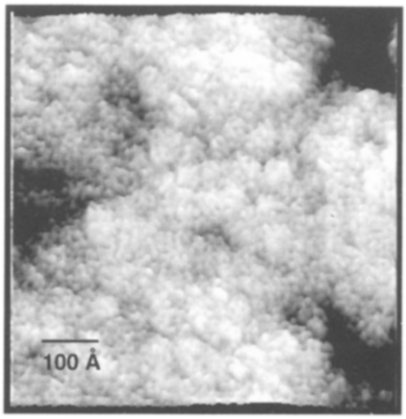

Fig. 8. High-resolution STM image of PbO_2 film from Fig. 7.

are evident. This is an interesting example of a repeating, self-similar (fractal) structure; the large grains are formed from smaller grains, etc. At higher resolution, features with a size of about 13 Å are resolved (Fig. 8).

Figure 9 shows several images of an electrodeposited PbO_2 film kept in the electrodeposition solution at open circuit. PbO_2 is soluble in the solution, so the changes in the images reflect the dissolution of the film. Here, the gray-scale offset of each image has been normalized to its average overall height. The image acquisition rate was about 12 s/image; six images from a larger set of images are shown. The small-grained material surrounding the edges of larger grains is etched preferentially, causing an apparent increase in the size of the large grains in the images. There is thermally-induced drift in the field of view of the microscope, to the 'northwest' direction. Features which track from image to image are indicated by the numbered arrows. The change in the structure of the grains, indicated by the arrows, occurs both because of etching of the tops of the grains, and exposure of the sides of the grains. During this process, the grains indicated by arrows 1 and 2 are dissolved. Similarly, the grains pointed to by arrows 3 and 4 change markedly, and the large grain indicated by arrow 5 also changes shape during observation, as the PbO_2 layer dissolves.

Conclusion

This preliminary study demonstrates that STM can be used to obtain real-space microstructural information about PbO_2. STM is a useful tool for investigating dynamic electrochemical phenomena, and high image acquisition rates improve the utility of STM for such work. The tomographic sectioning method is in the early stages of development, awaiting proper computer software for image manipulation. We are also experimenting with a generalized feature tracking method, to compensate for drift in the microscope's field of view. Knowledge of the effects of chemical environment and electrochemical deposition conditions on PbO_2 morphology will lead to better understanding of the properties of lead dioxide as battery electrode material. A more complete study of the influence of surfactants and electrochemical conditions on the nucleation and evolution of the microstructure of PbO_2 is envisioned.

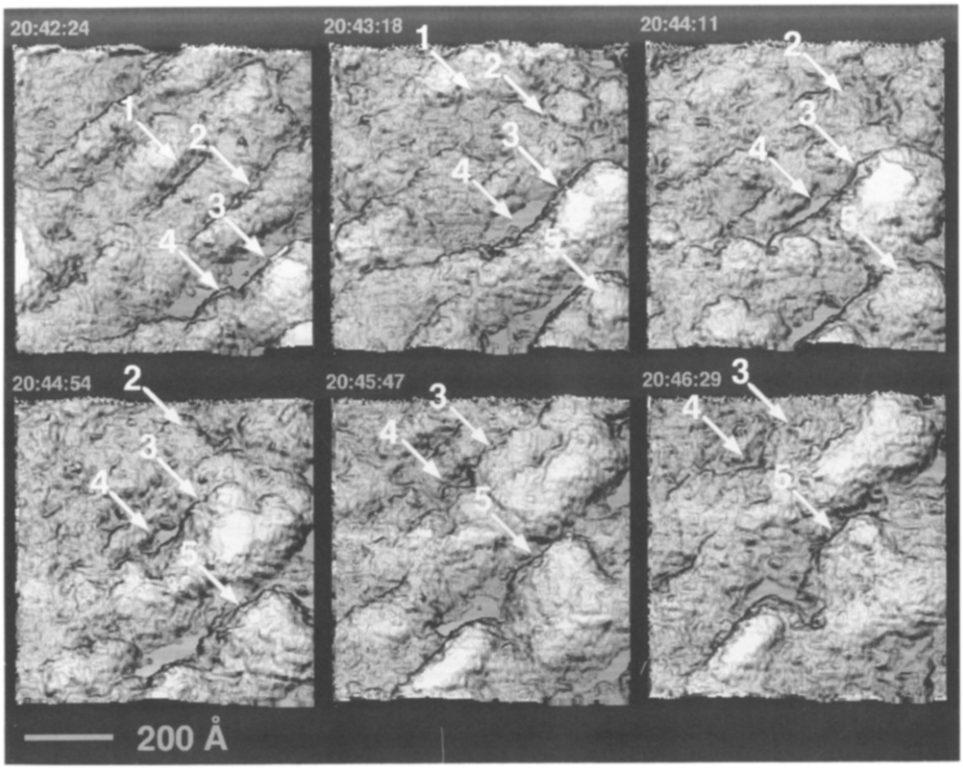

Fig. 9. *In situ* STM images of dissolving PbO_2 film on a platinum electrode. The numbered arrows track surface features which appear in each image. The features appear to move because of thermal drift in the microscope field of view. The time is indicated above each image.

References

1 G. Binnig, H. Rohrer, Ch. Gerber and E. Weibel, *Phys. Rev. Lett., 57* (1982) 49; G. Binnig and H. Rohrer, *Surf. Sci., 236* (1983) 126.

2 J. Tersoff and P. K. Hansma, *J. Appl. Phys., 61* (1987) R1.

3 G. Binnig and D. P. E. Smith, *Rev. Sci. Instrum., 57* (1986) 1688.

4 P. Lustenberger, H. Rohrer, R. Christoph and H. Siegenthaler, *J. Electroanal. Chem., 243* (1988) 225; M. P. Green, M. Richter, X. Xing, D. Scherson, K. J. Hanson, P. N. Ross, R. Carr and I. Lindau, *J. Microscopy, 152 Pt 3* (1988) 823; A. A. Gewirth and A. J. Bard, *J. Phys. Chem., 92* (1988) 5563; O. Lev, F. R. Fan and A. J. Bard, *J. Electrochem. Soc., 135* (1988) 783; J. Wiechers, T. Twomey, D. M. Kolb and R. J. Behm, *J. Electroanal. Chem., 248* (1988) 451; D. J. Trevor, C. E. D. Chidsey and D. N. Loiacono, *Phys. Rev. Lett., 62* (1989) 929.

5 R. S. Robinson, *J. Microscopy, 152 Pt 1* (1988) 541; R. S. Robinson, *J. Electrochem. Soc., 136* (1989) 3145; R. S. Robinson, *J. Vac. Sci. Technol. A, 8* (1990) 511.

6 G. Binnig, *Bull. Am. Phys. Soc., 30* (1985) 251; R. S. Becker, J. A. Golovchenko, D. R. Hamman and B. S. Swartzentruber, *Phys. Rev. Lett., 55* (1985) 2032; R. J. Hamers, R. M. Tromp and J. E. Demuth, *Phys. Rev. Lett., 56* (1986) 1972; W. J. Kaiser and R. C. Jaklevic, *IBM J. Res. Develop., 30* (1986) 411; R. M. Feenstra, J. A. Stroscio and A. P. Fein, *Surf. Sci., 181* (1987) 295; R. J. Hamers, Ph. Avouris and F. Bozso, *J. Vac. Sci. Technol. A, 6* (1988) 508; Ph. Avouris and R. Wolkow, *Phys. Rev. B, 39* (1989) 5091; J. A. Stroscio,

P. N. First, R. A. Dragoset, L. J. Whitman, D. T. Pierce and R. J. Celotta, *J. Vac. Sci. Technol. A, 8* (1990) 284; M. P. Everson, L. C. Davis, R. C. Jaklevic and W. Shen, *J. Vac. Sci. Technol. B, 9* (1991) 891.

7 R. S. Robinson and C. A. Widrig, *Langmuir, 8* (1992) 2311–2316.

8 B. A. Sexton, G. F. Cotterill, S. Fletcher and M. D. Horne, *J. Vac. Sci. Technol. A, 8* (1990) 544.

9 R. S. Robinson, *J. Microscopy, 152 Pt 2* (1988) 387; R. S. Robinson, T. H. Kimsey and R. Kimsey, *J. Vac. Sci. Technol. B, 9* (1991) 631; R. S. Robinson, T. H. Kimsey and R. Kimsey, *Rev. Sci. Instrum., 62* (1991) 1772.

10 R. S. Robinson, *J. Comp. Assist. Microscopy, 2* (1990) 53.

11 R. S. Robinson and R. L. McCreery, *J. Electroanal. Chem., 182* (1985) 61; R. M. Wightman and D. O. Wipf, in A. J. Bard (ed.), *Electroanalytical Chemistry*, Vol. 15, Marcel Dekker, New York, 1989, pp. 267–353; C. Amatore and C. Lefrou, *J. Electroanal. Chem., 296* (1990) 335.

12 T. Klitsner, R. S. Becker and J. S. Vickers, *Phys. Rev. B, 41* (1990) 3837.